Optimisation of HVOF Spray Process Parameters to Achieve Minimum Porosity and Maximum Hardness in WC-10Ni-5Cr Coatings

Pradeep Raj Rajendran [1,*] **, Thirumalaikumarasamy Duraisamy** [1] **, Ramachandran Chidambaram Seshadri** [2] **,
Ashokkumar Mohankumar** [3] **, Sathiyamoorthy Ranganathan** [4] **, Guruprasad Balachandran** [5] **,
Kaliyamoorthy Murugan** [6] **and Laxmi Renjith** [7]

[1] Department of Manufacturing Engineering, Annamalai University, Annamalai Nagar 608002, India;
tkumarasamy412@gmail.com

[2] Department of Materials Science and Engineering, The State University of New York (SUNY), Stony Brook,
New York, NY 11794, USA; csrcn1@gmail.com

[3] Department of Mechanical Engineering, Government College of Engineering, Bargur,
Krishnagiri 635104, India; ashokleadsaero12@gmail.com

[4] Department of Mechanical Engineering, Institute of Road Transport Polytechnic College, Bargur,
Krishnagiri 635104, India; rsmoorthy32@gmail.com

[5] Department of Mechanical Engineering, Alagappa Chettiar Government College of Engineering and
Technology, Karaikudi 63003, India; tellprasadcdm@gmail.com

[6] Department of Mechanical Engineering, Government Polytechnic College, Valangaiman,
Thiruvarur 612804, India; murugan.thermal@gmail.com

[7] Department of Mechanical Engineering, Mohandas College of Engineering and Technology,
Trivandrum 69554, India; laxmirenjith5@gmail.com

* Correspondence: krsreeraj1@gmail.com

Abstract: High-velocity oxy-fuel (HVOF) spray coating plays a major role in many surface treatment methods, which tend to improve erosion and corrosion resistance properties. HVOF is well known for its dense and high-quality coating ability. This is due to the less in-flight exposure time, which tends to have less oxide content because of its high-velocity properties. Among the number of process parameters, porosity and hardness are predominant factors while considering wear rate and corrosion behaviour analysis. The current study aims to optimise HVOF process parameters to obtain low levels of porosity and high hardness values in the WC-10Ni-5Cr coating sprayed on 35 Mo Cr steel. The flow rates of oxygen, LPG, coating powder feed rate and spray distance are selected in this study as these have a superior influence on the final condition of the coating. Statistical tools such as the design of experiments (DoE), analysis of variants and response surface methodology (RSM) were used to achieve the desired results. As per the result analysis, the oxygen flow rate has a higher effect on the porosity value and microhardness value of the coating.

Keywords: high-velocity oxy-fuel spraying; porosity; microhardness; response surface methodology

1. Introduction

Coatings have always played an essential role in empowering industries to fight problems of the early ruin of components that operate in severe environmental conditions. For a long time, coatings have been used to boost tribological performance, extend component life and durability and even enable the use of relatively cheaper substrate materials. Thermally sprayed coatings have some diverse advantages over other surface enhancement methods as they can be deposited over a wide range of thicknesses, even in complex geometries, without any constraints at lower costs. Thermal spray types such as high-velocity oxy-fuel (HVOF), atmospheric plasma spraying (APS) processes and cold spraying are now adopted by industries for developing coatings to battle against varied forms of surface degradation problems. Nowadays, more and more researchers are paying attention to

developing protective coatings for different systems to protect electrical equipment and to recover the operating capacity of the contact after its failure [1–7]. high-velocity oxy-fuel (HVOF) cermet coatings are broadly used in tribological applications, highlighting sliding conditions as the best substitute for hard chrome plating. The high wear resistance of these coatings is mostly due to their composite microstructure, composed of a carbide phase embedded into a ductile metal matrix. The carbides act as the reinforcing factor, and the metal binder increases the coating toughness and binds the carbide particles together. The HVOF process uses a supersonic jet flame formed by the burning of a mixture of oxygen and fuel. The decarburisation and oxidation in HVOF are less than in other conventional thermal spraying processes. This improves the properties such as low porosity and coating hardness of the sprayed coatings. The substrate is prepared to improve its adhesion to the coating. The substrate is first degreased and then sandblasted to enhance the surface roughness and accelerate the mechanical interlocking with the coating. The selection of fuels used in HVOF depends on the type of HVOF gun used and the coating to be deposited. Regularly, hydrogen, propane, kerosene (aviation grade) and liquefied petroleum gas (LPG) are used as fuels [8–10].

The HVOF spraying process could add the spray powder at supersonic speed to reach the substrate with high kinetic energy and enthalpy. With such a solid impact, the HVOF would have a fitted binding with the base metal, resulting in better low porosity, high hardness and bond strength in the micro-aspect. This successfully resolves wear- and corrosion-related problems [11]. High-velocity oxygen fuel (HVOF) thermal spraying is a substitute for hard chromium plating and/or conventional APS coatings in a range of situations. HVOF coatings exhibit lower porosity, high hardness, high bond strengths and lower roughness compared to APS coatings and are an environmentally friendly alternative to EHC. The current industry standard is to replace EHC with HVOF coatings. New nickel-chromium-based HVOF feedstock materials have shown promise for WC-based metal matrix composite coatings with superior corrosion resistance when used in marine applications. However, there is little information or data accessible on the corrosion and mechanical properties of such coatings, which is required before they can be used with assurance in real-world applications [12].

In this study, an approach has been made to optimise the process factors, such as oxygen and LPG flow rate, coating powder feed rate and distance between gun and base metal (spray distance), to obtain the minimum porosity level and maximum hardness of WC 10 Ni-5Cr coatings with HVOF technology. Tools such as DoE and RSM are used for level selection and to determine the contact effects between factors, which eliminates the drawback of orthodox methods, since in orthodox methods, a greater number of trials are required with sufficient time to determine the prime conditions [13].

2. Experimental Procedure and Methods

Here, WC-10Ni-5Cr cermet powder (WOKA-3552, Oerlikon Metco, Chennai, India) was selected as the coating material. From the scanning electron microscope (SEM), the analysis of the purchased powder shows the particle size in the range of −45 to 15 m (Figure 1a). The Electron Dispersive Spectrometer (EDS, Mitutoyo, Tokyo, Japan) confirms the chemical composition of the powder (Figure 1b). The substrate selected was commercially available 35CrMo Steel (ASTM A29/A29m) (AISI 4135), which is mainly used for the manufacturing of rolling mill gears, crankshafts, engine transmission parts and large motor shafts. EDS confirms the chemical composition of the substrate (Figure 1c). Tables 1 and 2 show the chemical composition of the substrate and coating powder.

WC-10Ni-5Cr powders are coated on 35CrMo substrate using HVOF Spraying facility found at Metallizing Equipment Co. Pvt. Ltd., Jodhpur, Rajasthan, Rajasthan, India (Gun: HIPOSET-2700) with a coating thickness of 250 microns. The thickness of the coating was observed with a micrometre (Digital) of 0.001 mm accuracy (Mitutoyo, Tokyo, Japan). The substrate was preheated before coating by one whole torch cycle with a pass velocity of 0.8 m/s at 120–180 °C. The specimen size used in this research is 50 mm × 40 mm ×

7 mm, and the number of samples prepared is 30 as per DOE (Table 3). Acetone is used for ultrasonic cleaning of samples and grit-blasted with corundum (320 ± 500 μm) to increase the surface roughness. The normal surface roughness was observed as 6 μm as per ASTM D7127-17 standards (Surface Roughness tester-Mitutoyo, Tokyo, Japan: Model Surf Test 301). Table 4 shows the process factors of WC-10Ni-5Cr coatings. Figure 2 shows the coated substrate material.

Table 1. Chemical composition of Substrate.

Percent	C%	Si%	Mn%	P%	S%	Cr%	Mo%
comp	0.35	0.2	0.602	0.015	0.012	0.972	0.205

Table 2. Chemical composition of coating powder.

Percent	C%	Cr%	Ni%	Fe%	W%
comp	5.4	5.03	10.25	0.06	Balance

Table 3. Experimental design matrix and result.

Sl. No	Coded Value				Original Value				Porosity (vol%)	Microhardness (HV)
	F	**O**	**S**	**L**	**F (gm/min)**	**O (slpm)**	**S (inch)**	**L (slpm)**		
1	−1	−1	−1	−1	35	240	6.5	50	2.87	792
2	1	−1	−1	−1	45	240	6.5	50	1.88	1060
3	−1	1	−1	−1	35	260	6.5	50	1.98	951
4	1	−1	−1	−1	45	260	6.5	50	1.72	1200
5	−1	−1	1	−1	35	240	7.5	50	3.49	790
6	1	−1	1	−1	45	240	7.5	50	3.11	864
7	−1	1	1	−1	35	260	7.5	50	1.76	1125
8	1	1	1	−1	45	260	7.5	50	1.93	1191
9	−1	−1	−1	1	35	240	6.5	60	3.25	850
10	1	−1	−1	1	45	240	6.5	60	1.3	1267
11	−1	1	−1	1	35	260	6.5	60	2.97	856
12	1	1	−1	1	45	260	6.5	60	2.1	1203
13	−1	−1	1	1	35	240	7.5	60	3.71	739
14	1	−1	1	1	45	240	7.5	60	3.2	736
15	−1	1	1	1	35	260	7.5	60	3.2	751
16	1	1	1	1	45	260	7.5	60	2.8	1021
17	−2	0	0	0	30	250	7	55	1.8	1155
18	2	0	0	0	50	250	7	55	3.56	860
19	0	−2	0	0	40	230	7	55	3.21	742
20	0	2	0	0	40	270	7	55	2.20	1198
21	0	0	−2	0	40	250	6	55	2.18	1042
22	0	0	2	0	40	250	8	55	3.25	875
23	0	0	0	−2	40	250	7	45	3.37	752
24	0	0	0	2	40	250	7	65	2.52	1068
25	0	0	0	0	40	250	7	55	1.62	1224
26	0	0	0	0	40	250	7	55	1.65	1192
27	0	0	0	0	40	250	7	55	1.61	1225
28	0	0	0	0	40	250	7	55	2.0	1262
29	0	0	0	0	40	250	7	55	1.52	1229
30	0	0	0	0	40	250	7	55	1.58	1238

Table 4. Parameters and possible working range of HVOF coating.

S. No	Parameters	Notations	Units	Levels				
				−2	−1	0	1	2
1	Powder feed rate	F	gm/min	30	35	40	45	50
2	Oxygen flow rate	O	slpm	230	240	250	260	270
3	Spray Distance	S	Inch	6	6.5	7	7.5	8
4	LPG flow rate	L	slpm	45	50	55	60	65
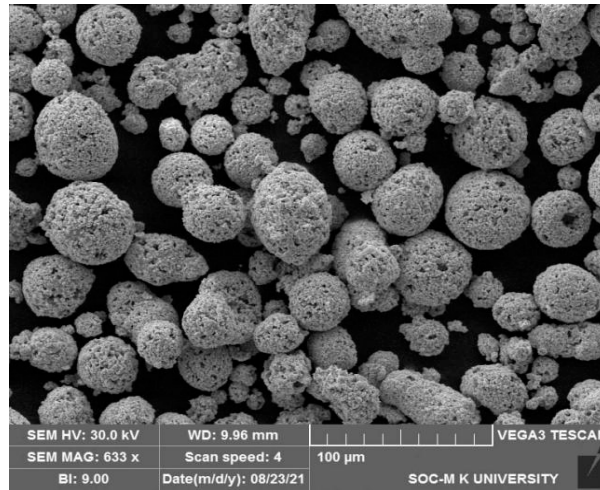
(**a**)
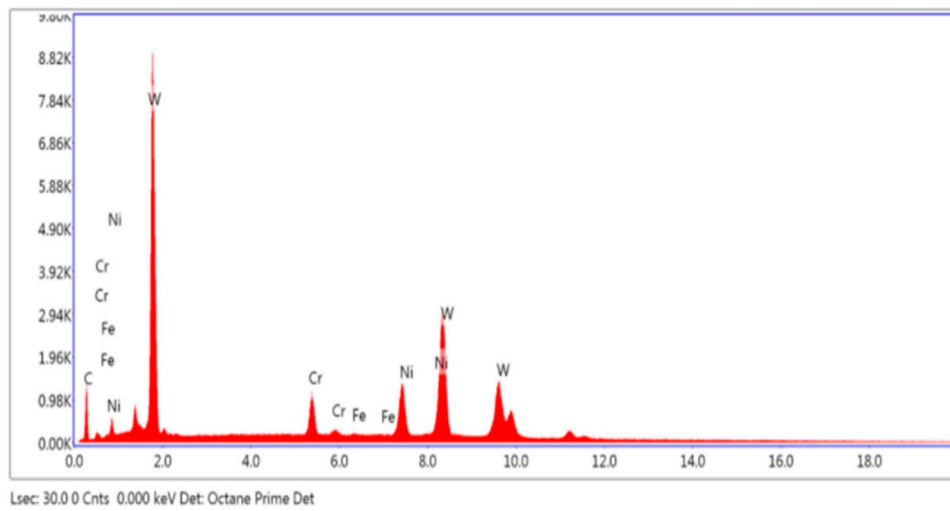
(**b**)

Figure 1. *Cont.*
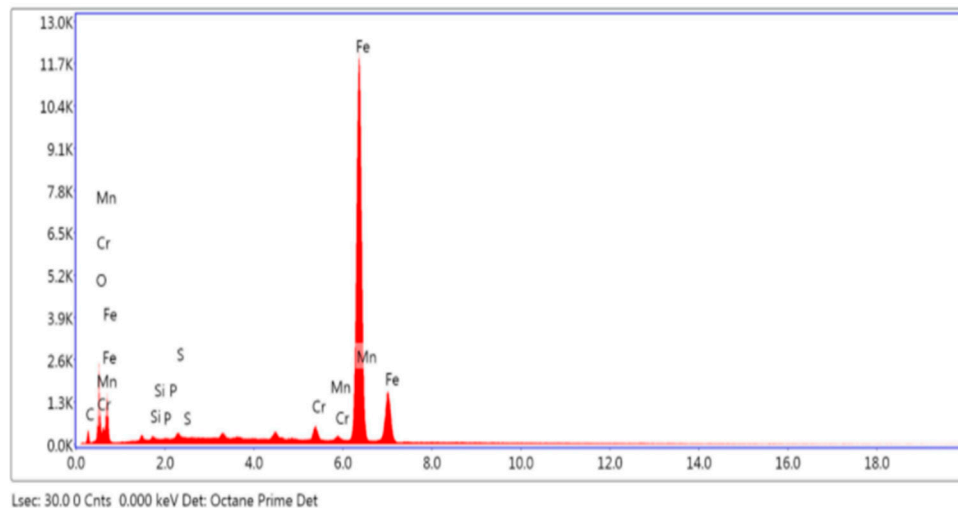
(**c**)

Figure 1. SEM micrograph of (**a**) received powder, (**b**) EDS of received powder and (**c**) EDS of base metal.

Published literature and laboratory investigations clearly state that factors such as fuel and gas flow rate, powder particle feed rate and spray distance have a huge impact on the act of HVOF coatings [14–19]. Thus, it is key to regulate the optimum conditions of the above factors to achieve low levels of porosity and maximum hardness. A sufficient number of experiments were scheduled by HVOF spraying of WC-10Ni-5Cr powders on 35CrMo Steel to evaluate the viable range of the above parameters by changing one of the factors separately. Necessary considerations are taken to avoid coating defects such as poor adhesion to the base metal, non-uniform melting of powder particles, the high value of porosity and surface cracks.

Figure 2 shows the HVOF coated substrate with WC-10Ni-5Cr powder. Figure 3 shows the SEM and EDS analysis of the coated material. Metallographic cross-sections of the coatings were prepared for the porosity measurements. The coated specimens were first cut to the specific dimensions using a wire-cut EDM (Model: Robocut 35; FANUC, Taiwan). They were then mounted with low viscosity epoxy resin in a vacuum environment. The mounted samples were continuously ground with 600, 800, 1000 and 211 1500 grit SiC papers and finally polished using diamond slurries of 10–8, 8–5, 5–2, 2–0.5 and 0.5–0 lm during 5, 5, 7, 10 and 10 min, respectively. Because of pull-outs in brittle materials, it is difficult to find and assess true porosity in a spray coating. If the metallographic grinding and polishing are not proper, it can cause artefacts that are not part of the coating. Ceramic coatings are brittle, and particles break off the surface during grinding. If not polished carefully, these breakouts leave an improper impression of porosity. The optical microscope (Make: Meiji; Tokyo, Japan, Model: MIL-7100) equipped with an image analysis system (Metal Vison Version.6), according to ASTM B 276, was used to measure the porosity of the metallographically prepared cross-sections of the coating. For this study, images collected with optical spectroscopy below 1000× were handpicked for porosity analysis to view image attributes such as pores that are open and a regular network of cracks. Initially, a four-hundred-micron square region was selected on the polished cross-section of the coating, and the image was also analysed. The experiment was repeated at five different spots to achieve the average percentage value of the amount of porosity. Microhardness measurements were conducted by indenting the metallographic cross-sections under a 300 g load for 15 s using a Vickers microhardness tester (Make: Shimadzu, Tokyo, Japan; Model: HMV-2T). For each coating sample, the measurement series comprised 20 random indentations. The distance between indentations was kept three times longer than the indentation diagonal to prevent the effects of the stress field of nearby indentations.

Here, RSM with CCD is used with the full replication method. The four main factors (F, O, S, L) were selected based on the previous literature results. Five different stages of the variables and values are shown in Table 4.
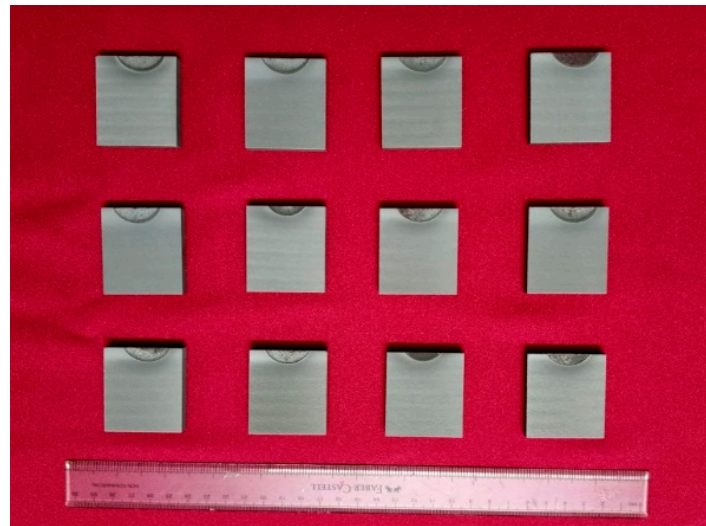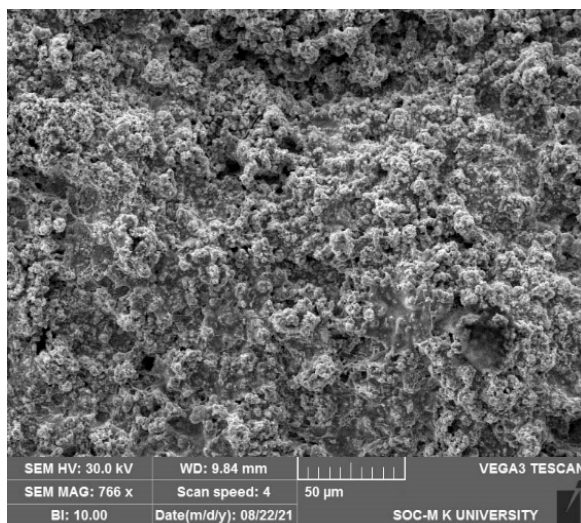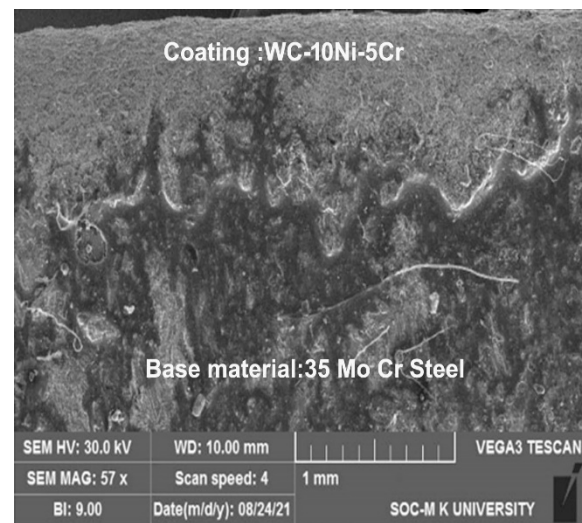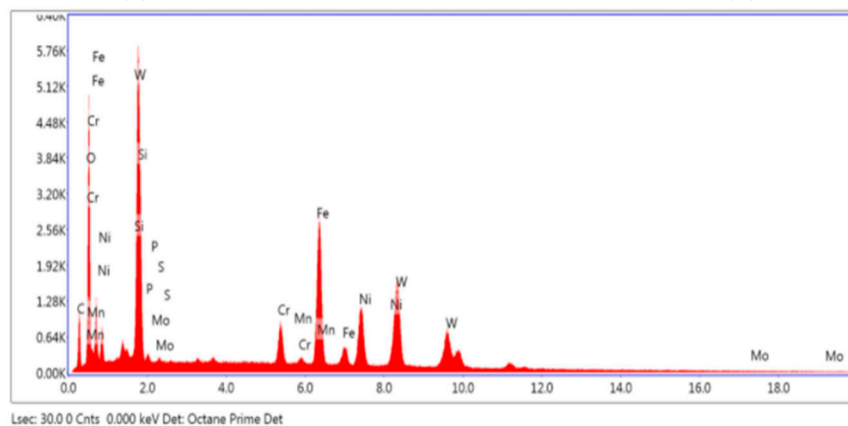

Figure 2. Coated substrate.
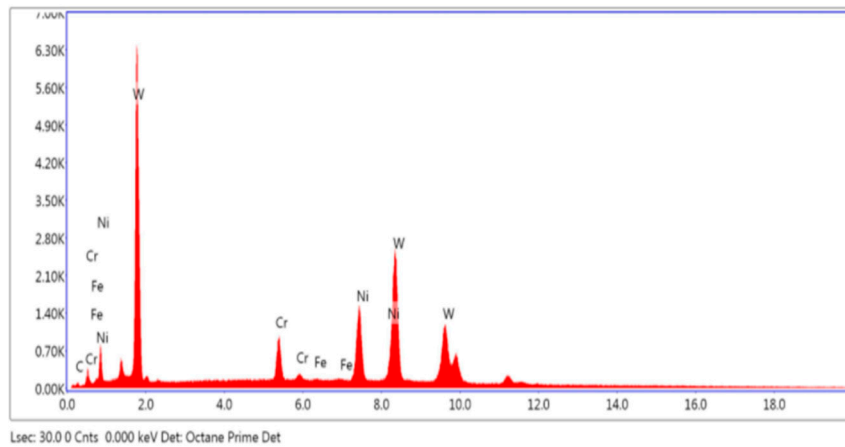

(**a**)

(**b**)

(**c**)

Figure 3. *Cont.*

(**d**)

Figure 3. SEM micrograph of HVOF-coated (**a**) top surface, (**b**) cross-section, (**c**) EDS of top surface and (**d**) EDS of cross-section.

3. Developing Empirical Relationships

RSM is used to relate the HVOF spray parameters and coating features. RSM is an exact and numerical tool that is usually used for DoE in order to develop mathematical models, optimise initial factors and obtain a graphical model of results that help for clear analysis.

The following regression equation is used to signify the relationship between the variable and the responses [20,21]:

$$Y = B_0 + \sum B_I X_I + \sum B_{II} X_I^2 + B_{IJ} X_I X_J \tag{1}$$

where Y and X_I, X_I^2 and X_J are the predicted and variables in coded value; B_O, B_I, B_{II} and B_I are the constant, linear effect, squared effect and interaction effect, respectively.

Table 4 gives the reasonable limit of HVOF spray parameters. Here, four variables are selected for analysis. Therefore, put K = 4. Here, 30 trials were performed as per the design shown in Table 3. Table 5 shows the experimental conditions and images for experimental responses of feasible working ranges.

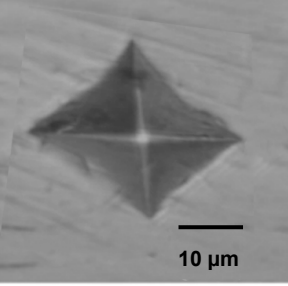**Table 5.** Trial conditions and images for experimental responses.

Spray Trials	Microstructure for Porosity Analysis	Binary Image for Porosity Analysis	Microhardness Indentation
No:1 F = 35 gpm O = 240 lpm S = 6.5 Inch L = 50 lpm			

Table 5. *Cont.*
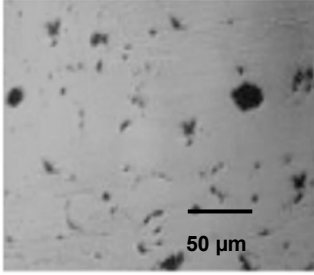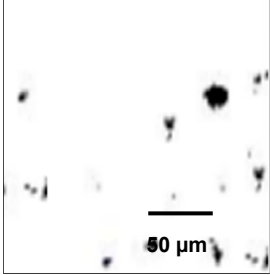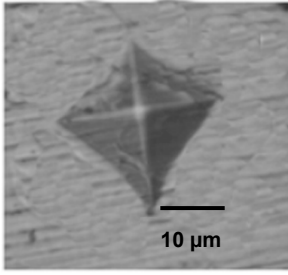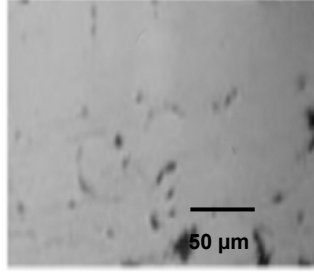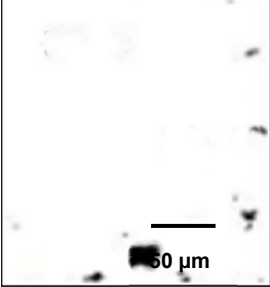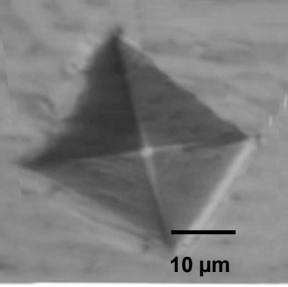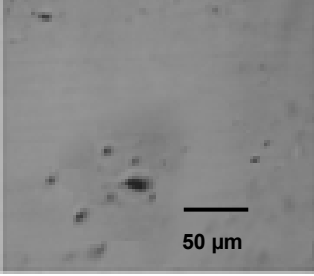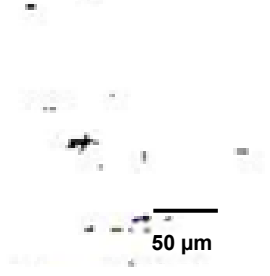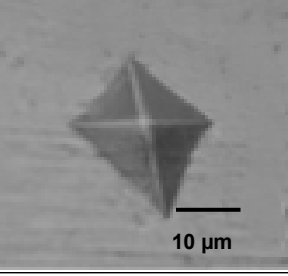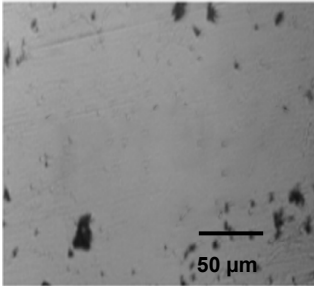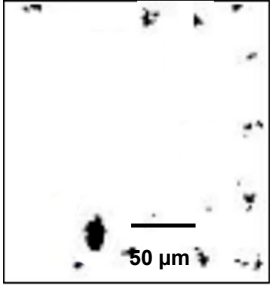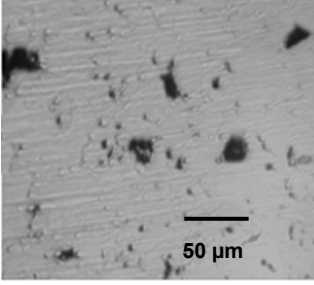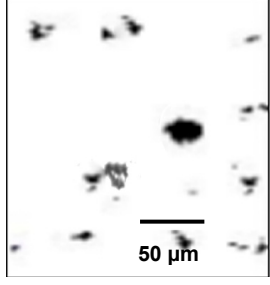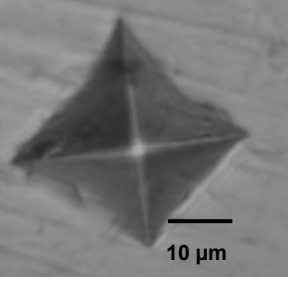
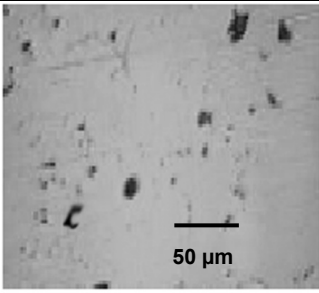| Spray Trials	Microstructure for Porosity Analysis	Binary Image for Porosity Analysis	Microhardness Indentation
No:2 F = 45 gpm O = 240 lpm S = 6.5 Inch L = 50 lpm			
No:3 F = 35 gpm O = 260 lpm S = 6.5 Inch L = 50 lpm			
No:4 F = 45 gpm O = 260 lpm S = 6.5 Inch L = 50 lpm			
No:5 F = 35 gpm O = 240 lpm S = 7.5 Inch L = 50 lpm			
No:6 F = 45 gpm O = 240 lpm S = 7.5 Inch L = 50 lpm			

Table 5. *Cont.*
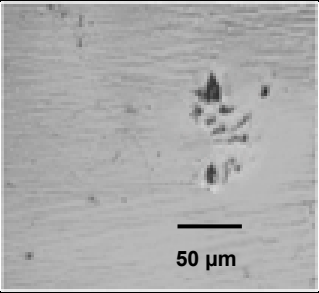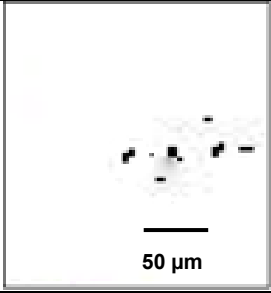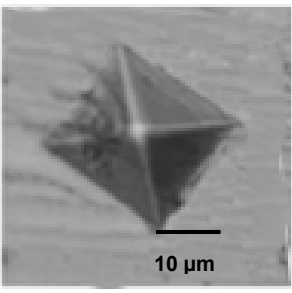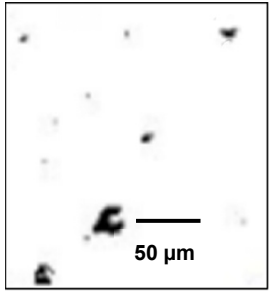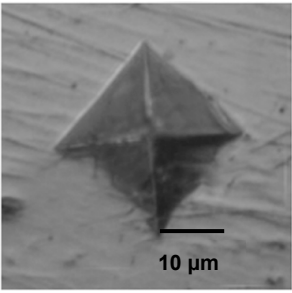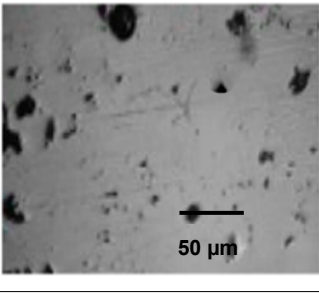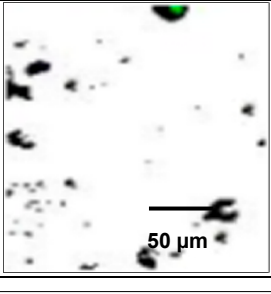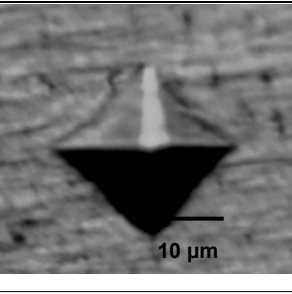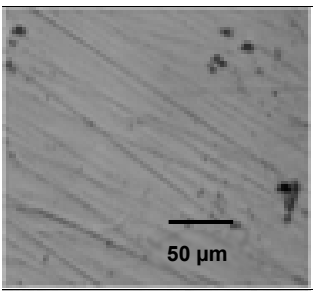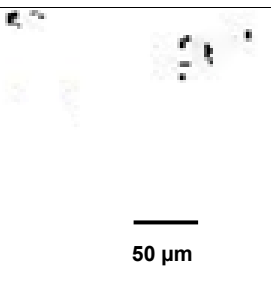
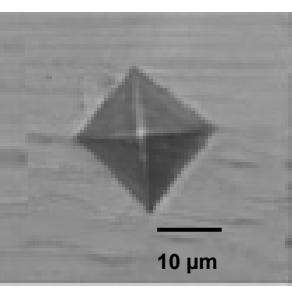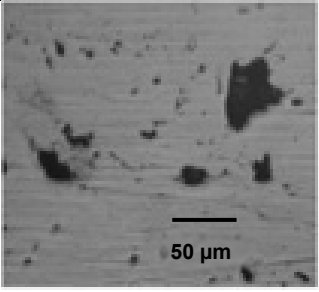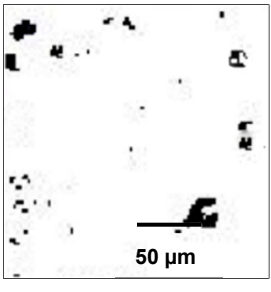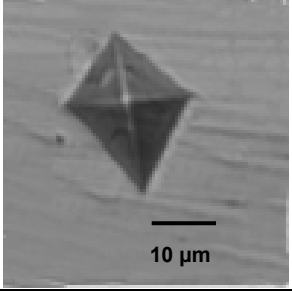| Spray Trials	Microstructure for Porosity Analysis	Binary Image for Porosity Analysis	Microhardness Indentation
No:7 F = 35 gpm O = 260 lpm S = 7.5 Inch L = 50 lpm			
No:8 F = 45 gpm O = 260 lpm S = 7.5 Inch L = 50 lpm			
No:9 F = 35 gpm O = 240 lpm S = 6.5 Inch L = 60 lpm			
No:10 F = 45 gpm O = 240 lpm S = 6.5 Inch L = 60 lpm			
No:11 F = 35 gpm O = 260 lpm S = 6.5 Inch L = 60 lpm			
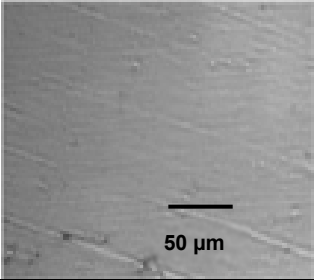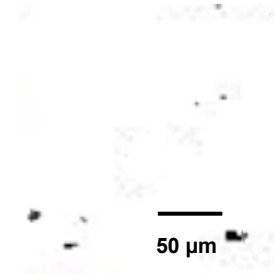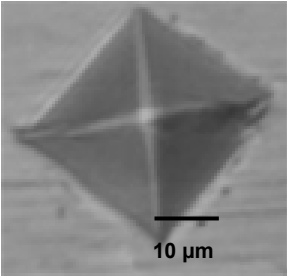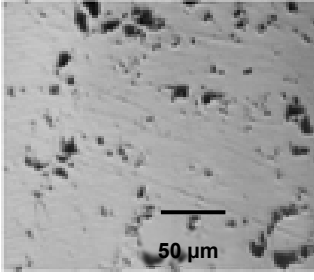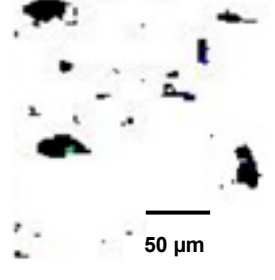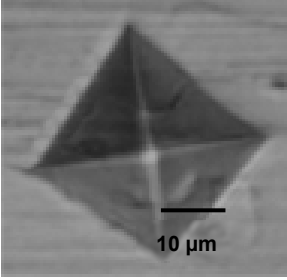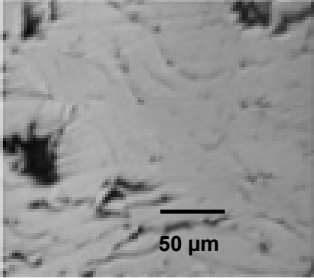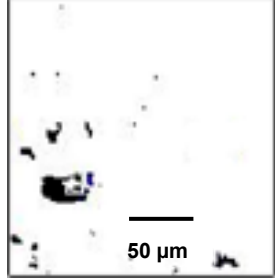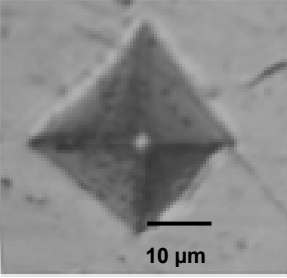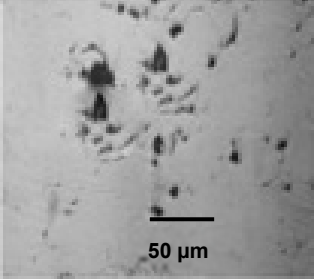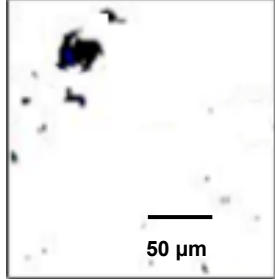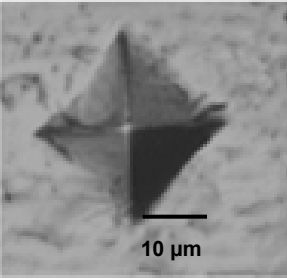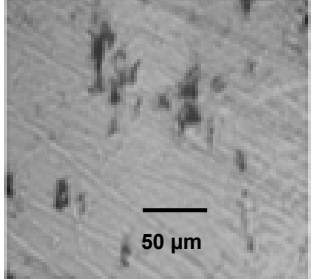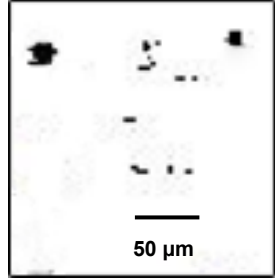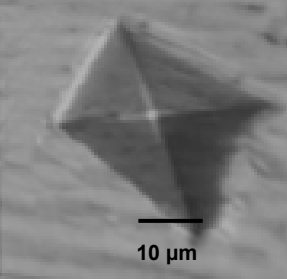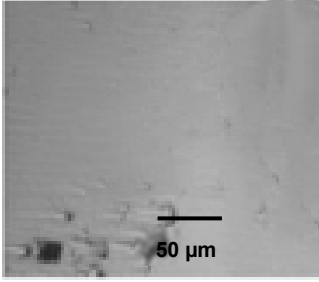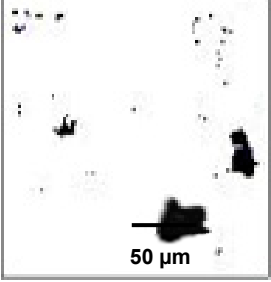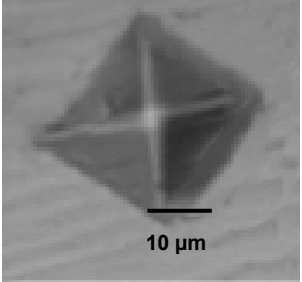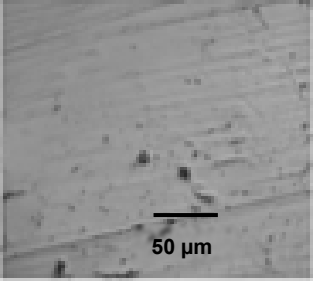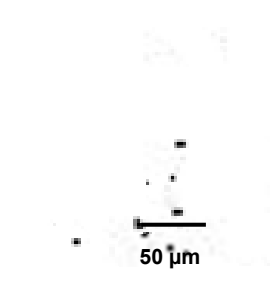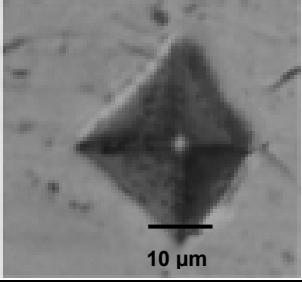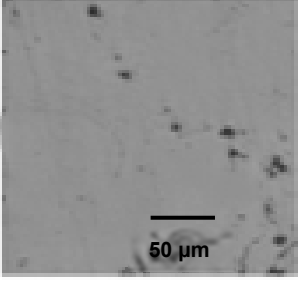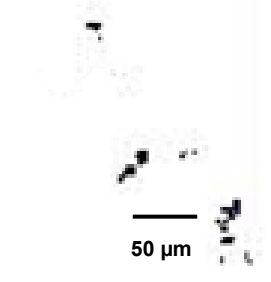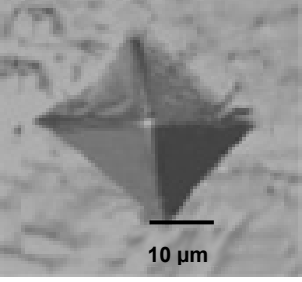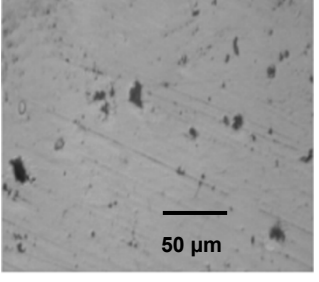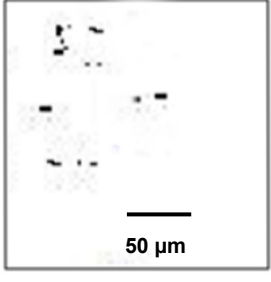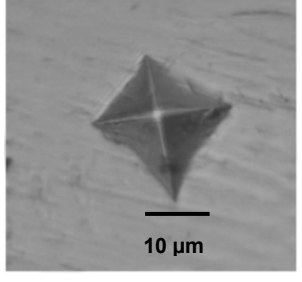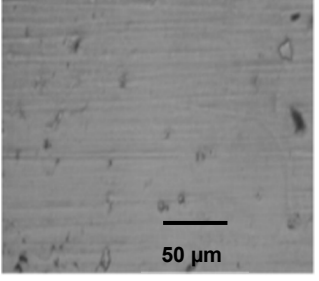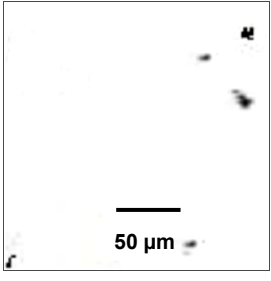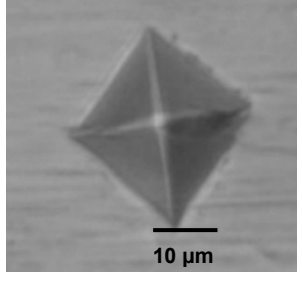
Table 5. *Cont.*

Spray Trials	Microstructure for Porosity Analysis	Binary Image for Porosity Analysis	Microhardness Indentation
No:12 F = 45 gpm O = 260 lpm S = 6.5 Inch L = 60 lpm			
No:13 F = 35 gpm O = 240 lpm S = 7.5 Inch L = 60 lpm			
No:14 F = 45 gpm O = 240 lpm S = 7.5 Inch L = 60 lpm			
No:15 F = 35 gpm O = 260 lpm S = 7.5 Inch L = 60 lpm			
No:21 F = 40 gpm O = 250 lpm S = 6 Inch L = 55 lpm			

Table 5. *Cont.*

Spray Trials	Microstructure for Porosity Analysis	Binary Image for Porosity Analysis	Microhardness Indentation
No:22 F = 40 gpm O = 250 lpm S = 8 Inch L = 55 lpm	 50 µm	 50 µm	 10 µm
No:23 F = 40 gpm O = 250 lpm S = 7 Inch L = 45 lpm	 50 µm	 50 µm	 10 µm
No:24 F = 40 gpm O = 250 lpm S = 7 Inch L = 65 lpm	 50 µm	 50 µm	 10 µm
No:25 F = 10 gpm O = 250 lpm S = 7 Inch L = 55 lpm	 50 µm	 50 µm	 10 µm
No:26 F = 10 gpm O = 250 lpm S = 7 Inch L = 55 lpm	 50 µm	 50 µm	 10 µm

The microhardness and porosity of the HVOF sprayed coating are the dependent variables of the powder particle feed rate (F), flow rate of oxygen (O), spray distance (S) and flow rate of LPG(L).

This is conveyed as

$$\text{Response} = f\,(F, O, S, L) \tag{2}$$

For the selected above factors, the polynomial equation can be stated as

$$
\begin{aligned}
Y = b_o &+ b_1(F) + b_2(O) + b_3(S) + b_4(L) + b_{11}(FO) + b_{12}(FS) + b_{13}(FL) + b_{23}(OS) + b_{24}(OL) + b_{34}(SL) \\
&+ b_{11}(F^2) + b_{22}(O^2) + b_{33}(S^2) + b_{44}(L^2)
\end{aligned} \tag{3}
$$

where b_o, b_1, b_2, b_3, ... , b_{nn} are the middling responses and regression coefficients that hinge on respective linear, interaction and squared terms of factors.

4. Results and Discussion

'*p*' values and Student's *t*-test are used to calculate the significance of the respective coefficient in Tables 3 and 4.

Here, F, O, S, L, FO, FS, FL, OS, OL, SL, F^2, O^2, S^2 and L^2 are taken as significant model terms. The values of "Prob > F' less than 0.5 display that the model terms are important. The final empirical relationship was recognised with these significant coefficients.

For coating porosity:

$$
\begin{aligned}
[305.61833 &- 1.11692(F) - 1.39146(O) - 8.57883(S) - 2.77475(L) + 0.603088(FO) + 0.073750(FS) \\
&- 0.005685(FL) - 0.041125(OS) + 0.004462(OL) + 0.036250(SL) + 0.001221(F^2) + 0.002568(O^2) + 1.03708(S^2) \\
&+ 0.015071(L^2)]\ \text{vol.\%}
\end{aligned} \tag{4}
$$

For microhardness:

$$
\begin{aligned}
[68{,}167.45833(F) &+ 275.75833(O) + 2525.25000(S) + 708.78333(L) + 0.121250(FO) - 28.17500(FS) + 0.737500(FL) \\
&+ 12.13750(OS) - 0.803750\,(OL) - 16.07500(SL) - 1.64708(F^2) - 0.623021(O^2) - 260.70833(S^2) \\
&- 3.88208(L^2)]\ \text{HV}
\end{aligned} \tag{5}
$$

The least probability value in Fisher's F-test gives a good regression model in order to calculate the hardness and porosity. The determination coefficient (R^2) is used to evaluate the goodness of fit. From the results, the R^2 values for the porosity and microhardness are 0.9771 and 0.9821. This shows that 97.71% and 98.21% of the investigational values are compatible with the desired results. An R^2 value close to 0.1 indicates a good statistical model for the analysis.

From Figure 4, the errors are normally distributed, and the observed values match with its experimental values healthily (Correlation Graph).

Here, porosity and microhardness are the two parameters chosen as a response for numerical and pictorial/graphical optimisation analysis. Because of the inverse relationship between porosity and hardness of the HVOF coating [22], efforts were made to maximise the surface hardness while minimising the porosity to obtain an optimised value. Microhardness and porosity are the dependent variables, and the flow rate of fuel and gas, powder feed rate and spray distance are the independent variables selected for applying constraints to develop the optimised condition. Porosity levels were estimated and plotted in Figure 5 as per Equation (4).

Three-dimensional graphs were calculated under assured process settings to check the nature of process factors on hardness and porosity levels. Contour plots are used to search visually for the apt value; from Figure 5, the porosity level shows down and up with the increase in powder feed rate, spray distance and LPG flow rate. The minimum porosity is given by the valley of the response plot, and these response contours are used to determine the porosity in any region of the experimental area. A contour plot always helps to understand the minimum, maximum or saddle point response from a stationary point, which is observed by virtual observation of the response [23].

From Figure 6, it is clear that the carrier's gas flow rate (O) plays a major role in the coating hardness on a micro-level. The thermally energised flame in HVOF increases with a rise in the oxygen flow rate. On account of the high thermal energy of the coating, the

particles melt effectively, which results in a good coating on the substrate. This helps to form a coating with minimum porosity and good adhesion strength. However, the further rise in oxygen flow rate resulted in higher porosity and lower bond strength. This is due to the lowering of flame temperature, which results in less melting of coating powder particles [2]. Studies stated that the particle size of the powder also affects the coating hardness, wear and corrosion resistance. A lower particle size will improve the coating properties due to better melting of powder particles with a moderate level of oxygen flow rate [24].

From the results, at low and high LPG flow rates, the volume percentage of porosity is higher than at the intermediate level. A higher fuel flow rate results in higher power output. The higher chamber pressure created due to the higher fuel flow rate increased the particle velocity. This is due to the boosted viscosity of gas and higher momentum interaction between the particles and gas phase [25]. Hammering effects are created on the coating surface when particles impact at a high velocity. This creates a high porosity level in the coating due to the bouncing off of the particles from the deposited surface.

According to the regression Equation (5), Figure 6 gives the three-dimensional response surface plots of coating hardness. From Figure 6, it is well clear that the coating hardness shows an increased nature and then decreases after attaining a minimum value with the increase in particle feed rate, flow rate of oxygen, spray distance and flow rate of LPG. The maximum microhardness value is given by the peak point in the response plot. The powder feed rate shows an inverse relationship with microhardness and is directly proportional to the percentage of porosity.

At low and high stages of particle feed rate result in vaporisation of powder or improper melting of the particles. Due to this, porosity maximises, and hardness minimises.

When considering the effect of spray distance (S), lowering the spray distance results in a massive change (increase) in the porosity level and minimises the hardness. This is due to the variation of the kinetic value of the propagated particles. It is observed that a good result was found for middle values of spray distance. From these observations, we find a multi-objective strategy is necessary to meet the defined objectives.

To attain such a result, a multi-objective way of optimisation is selected. Figure 7 shows the overlay relations of the porosity and microhardness for the predicted formulations. The layout grey shades stand for the maximum microhardness and minimum porosity values.

(a)   (b)
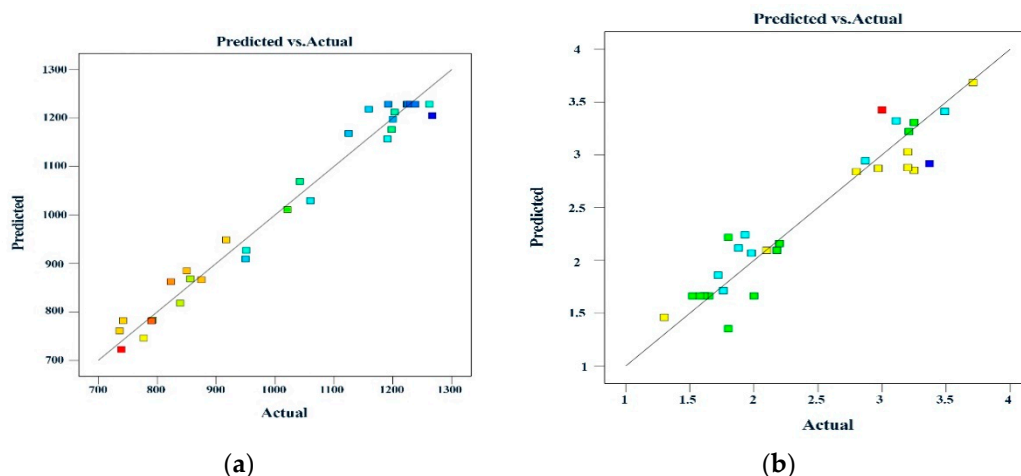
Figure 4. The Correlation Graph for (**a**) Porosity vol% (**b**) Hardness HV.
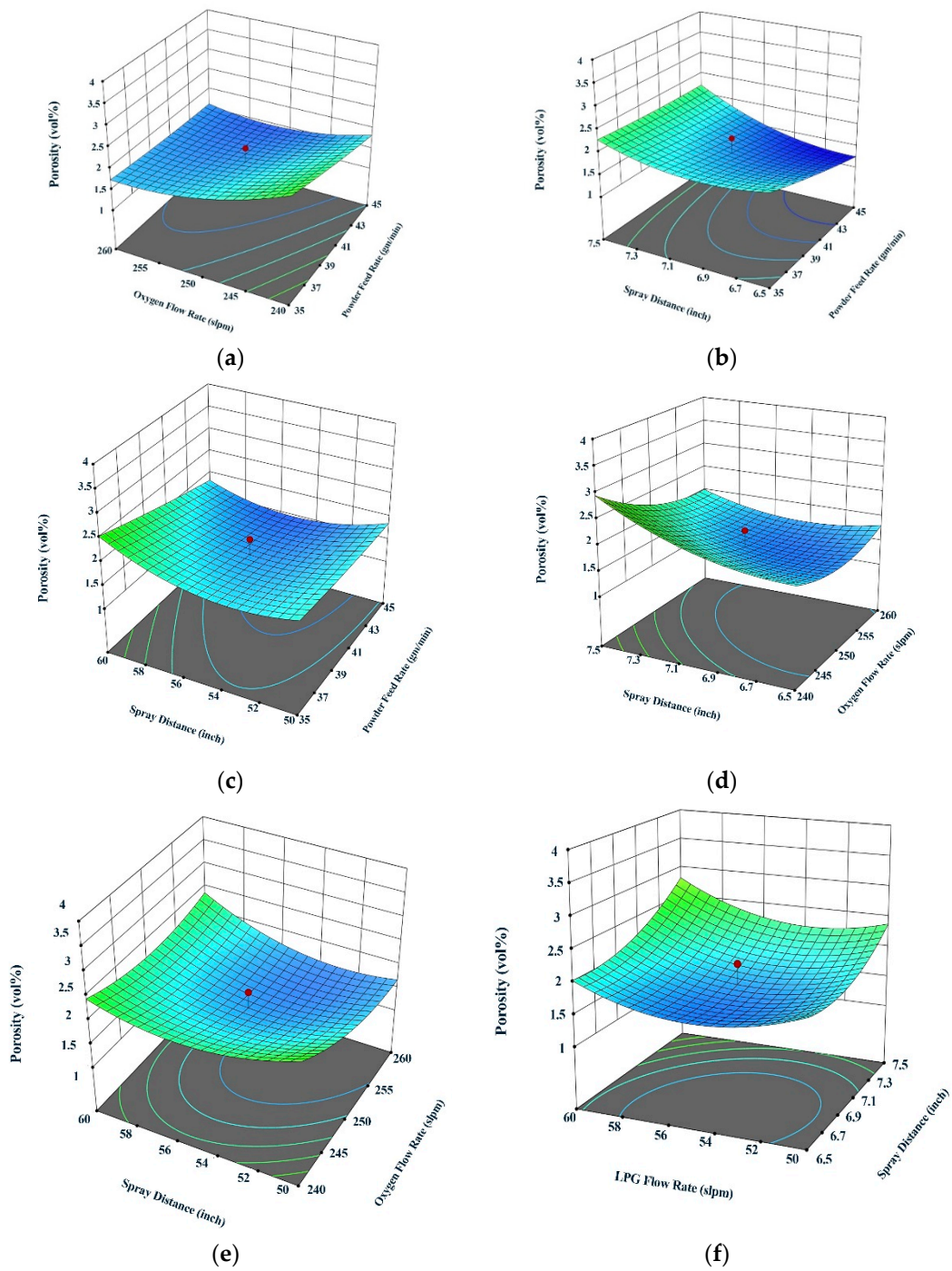
Figure 5. Response graph for the effect of parameters coating porosity: (**a**) F and O; (**b**) F and S; (**c**) F and L; (**d**) O and S; (**e**) O and L; (**f**) S and L.
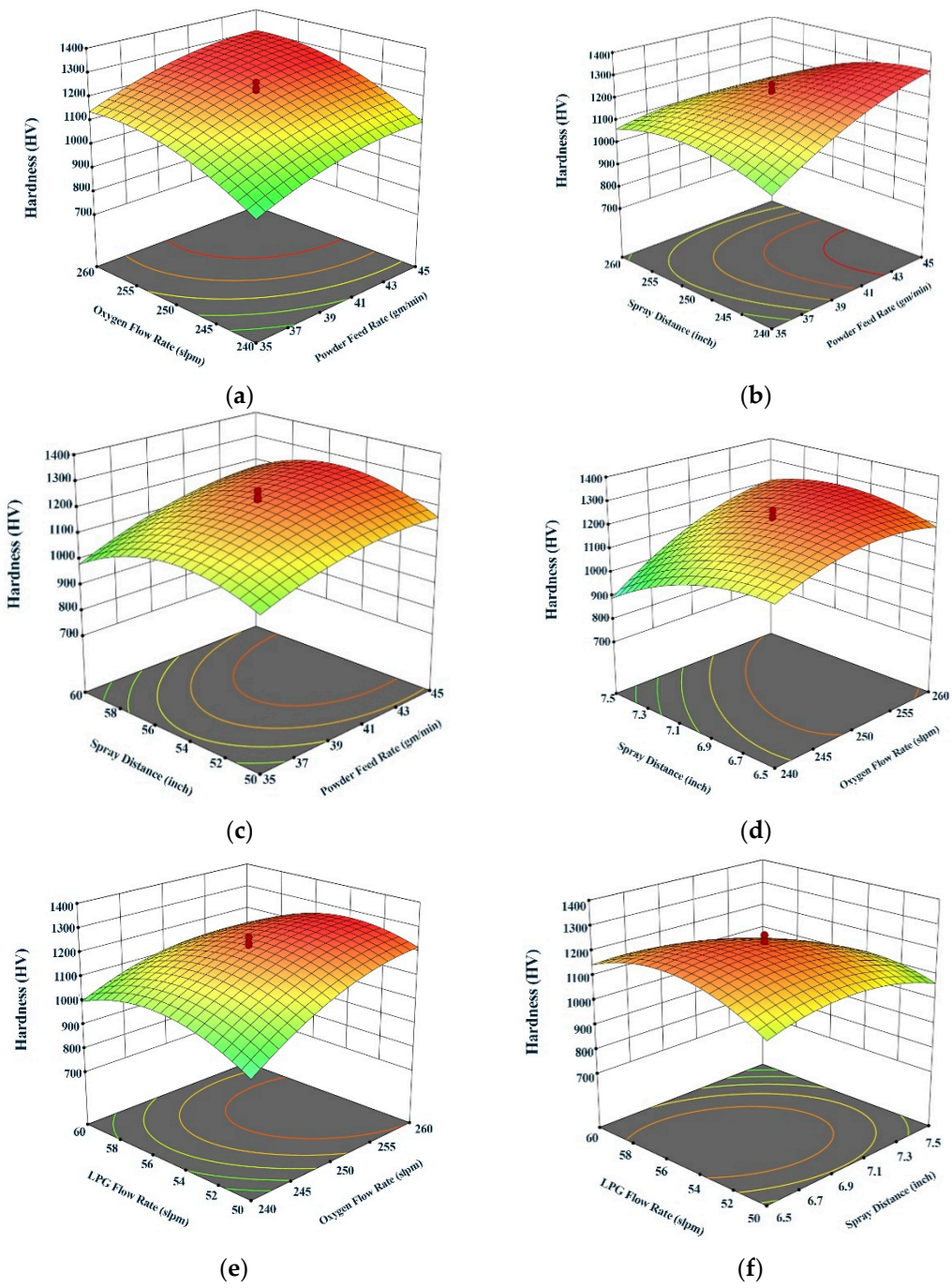
Figure 6. Response graph for the effect of parameters on coating hardness: (**a**) F and O; (**b**) F and S; (**c**) F and L; (**d**) O and S; (**e**) O and L; (**f**) S and L.

(**a**) (**b**)
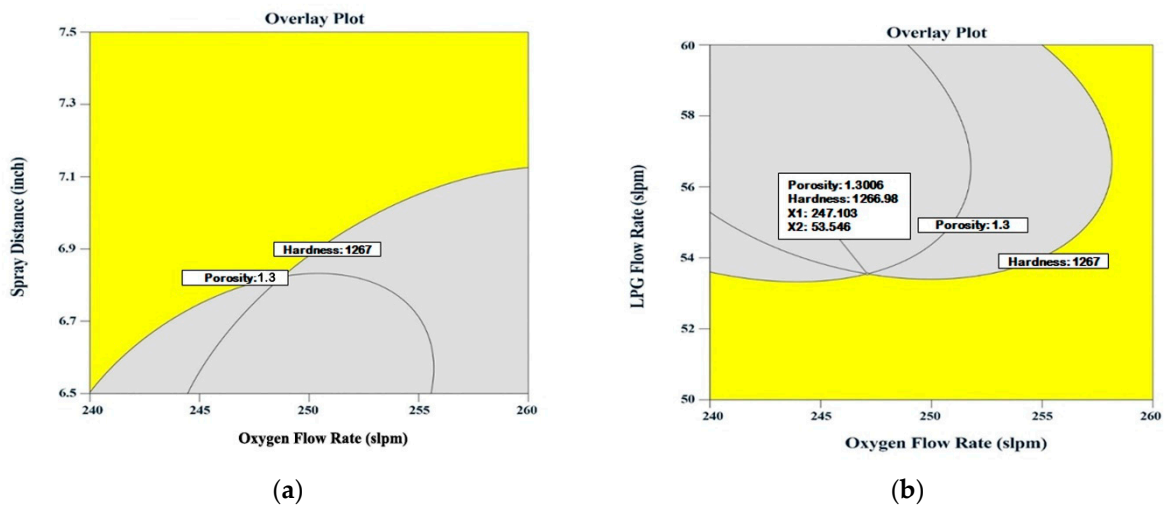
Figure 7. Overlay plots of optimised HVOF coating parameters to achieve minimum porosity and maximum microhardness. (**a**) Interaction between Oxygen flow rate and Spray distance, (**b**) Interaction between Oxygen flow rate and LPG flow rate.

5. Confirmation and Validation

5.1. Authentication of Developed Empirical Relationships

In order to check whether the established relationship calculates the reactions exactly, more experiments are performed using spray process factors but are not included in Table 4. Tables 6 and 7 show the predicted and experimental values of porosity and hardness found using established relations. It is found that variations between predicted and experimental values are within ±5%. Thus, the developed relationships can be used resourcefully to determine the levels of porosity and hardness of HVOF-coated WC-10Ni 5Cr with a confidence level of 95%.

Table 6. ANOVA values for the response coating porosity.

Source	Sum of Squares	df	Mean Square	F-Value	*p*-Value	
Model	14.36	14	1.03	10.35	<0.0001	Significant
F-powder feed rate	1.12	1	1.12	11.33	0.0042	
O-oxygen flow rate	1.69	1	1.69	17.06	0.0009	
S-spray distance	2.2	1	2.2	22.23	0.0003	
L-LPG flow rate	0.3876	1	0.3876	3.91	0.0666	
FO	0.3813	1	0.3813	3.85	0.0686	
FS	0.5439	1	0.5439	5.49	0.0333	
FL	0.3221	1	0.3221	3.25	0.0915	
OS	0.6765	1	0.6765	6.83	0.0196	
OL	0.7966	1	0.7966	8.04	0.0125	
SL	0.1314	1	0.1314	1.33	0.2675	
F^2	0.0256	1	0.0256	0.2579	0.619	
O^2	1.81	1	1.81	18.25	0.0007	
S^2	1.84	1	1.84	18.61	0.0006	
L^2	3.89	1	3.89	39.3	<0.0001	
Residual	1.49	15	0.0991			
Lack of fit	1.34	10	0.134	4.6	0.053	Not significant
Pure error	0.1457	5	0.0291			Cor total: corrected total
Cor total	15.85	29				PRESS: predicted error sum of squares
Std. dev = 37.94		R^2 = 0.9772				df: degrees of freedom
Mean = 1018.24		Adj R^2 = 0.9364				CV: coefficient of variation
C.V.% = 3.75		Pred R^2 = 0.8602				F: Fisher's ratio
PRESS = 1.14×10^5		Adeq Precision = 18.155				p: probability

Table 7. ANOVA values for the response coating hardness.

Source	Sum of Squares	df	Mean Square	F-Value	*p*-Value	
Model	1.03×10^6	14	73,333.46	43.07	<0.0001	Significant
F- powder feed rate	1.43×10^5	1	1.43×10^5	84.04	<0.0001	
O- oxygen flow rate	2.33×10^5	1	2.33×10^5	136.89	<0.0001	
S-spray distance	6.17×10^4	1	61,712.04	36.25	<0.0001	
L-LPG flow rate	2.93×10^3	1	2926.04	1.72	0.2096	
FO	5.88×10^2	1	588.06	0.3454	0.5655	
FS	7.94×10^4	1	79,383.06	46.63	<0.0001	
FL	5.44×10^3	1	5439.06	3.19	0.0941	
OS	5.89×10^4	1	5.89×10^4	34.61	<0.0001	
OL	2.58×10^4	1	2.58×10^4	15.18	<0.0014	
SL	2.58×10^4	1	$2.58 x10^4$	15.18	<0.0014	
F^2	4.65×10^4	1	4.65×10^4	27.32	0.0001	
O^2	1.07×10^5	1	1.07×10^5	62.54	<0.0001	
S^2	1.17×10^5	1	1.17×10^5	68.44	<0.0001	
L^2	2.58×10^5	1	2.58×10^5	151.75	<0.0001	
Residual	2.55×10^4	15	1.70×10^3			
Lack of fit	2.30×10^4	10	2.30×10^3	4.45	5.65×10^{-2}	Not significant
Pure error	2.58×10^3	5	5.15×10^2		Cor total: corrected total	
Core total	1.05×10^6	29			PRESS: predicted error sum of squares	
Std. dev = 37.93		R^2 = 0.9771			df: degrees of freedom	
Mean = 1018.23		Adj R^2 = 0.9364			CV: coefficient of variation	
C.V.% = 3.73		Pred R^2 = 0.8602			F: Fisher's ratio	
PRESS = 1.147×10^5		Adeq Precision = 18.155			p: probability	

5.2. Affiliation between Porosity and Hardness

When the level of micro cracks and porosity in the sprayed coating is minimised, the hardness of the coating increases. The following regression equation is governed by the nature of the graph:

$$\text{Microhardness (HV)} = 1498.9 - 222.75 \text{ (Porosity in vol\%)} \tag{6}$$

The negative nature of the slope of the regression equation specifies that porosity and microhardness show an inverse relationship.

The value of determination coefficient R^2 = 86.94% shows the degree of goodness of fit of the given calculations. Here, values of R^2 are in the range between 0 and 1, which clearly shows the fit of the established empirical relationships based on empirical conditions. The obtained R^2 value helps to conclude that the regression model has a good capability to predict the porosity level and hardness.

5.3. Justification of Optimisation Procedures

Depending on the outcomes gained by the analysis, the suggested optimum parameters are shown in Table 8. HVOF experiments were planned and conducted with these factors, and additional sets of trials were also performed with high and low levels of optimised conditions, as presented in Table 9.

The results show that deviating from the optimised spray conditions increases coating porosity while decreasing coating hardness due to a lack of energy supplied to powder particles by the HVOF flame, variations in in-flight time and variations in spray distance.

Table 8. Authentication of results for developed empirical relationships.

Expt.No	HVOF Spray Parameters				Coating Porosity (Vol%)			Coating Microhardness (HV)		
	Powder Feed Rate (gm/min)	Oxygen Flow Rate (slpm)	Spray Distance (inch)	LPG Flow Rate (slpm)	By Experiment	By Modal	Variation (%)	By Experiment	By Modal	Variation (%)
1	30	230	6	50	1.55	1.6	+3.13	1222	1276	+4.23
2	35	250	7	55	1.86	1.8	−2.78	1186	1202	+1.33
3	45	270	8	60	2.2	2.1	−4.76	1310	1255	−4.38

Table 9. Authentication of results for optimisation procedure.

Expt.No.	HVOF Spray Parameters				Coating Porosity (Vol%)	Coating Microhardness (HV)
	Powder Feed Rate (gm/min)	Oxygen Flow Rate (slpm)	Spray Distance (inch)	LPG Flow Rate (slpm)		
1	48	247	6	54	1.3	1267
2	45	244	5.5	51	1.9	1061
3	51	250	6.5	57	2.3	900

5.4. Investigation of Optimised Coating

A large value of tungsten monocarbide (WC) was found on the coating developed with optimised HVOF parameters. The coating also has good adhesion to the base metal, with few cracks at the base metal's boundary. A dense coating gives a minimum level of porosity with maximum hardness. Recommended particle size and optimised processing parameters make it easy to achieve good surface malting of particles during in-flight [26,27]. This results in a good, desired splat formation. Thus, the probability of getting a coating with the least porosity and hardness is increased. This is also due to the retention of WC in the coating [20].

6. Conclusions

1. WC-10Ni-5Cr coatings on 35Cr Mo Steel with HVOF were performed to evaluate the optimum spray conditions to achieve the minimum and maximum level of porosity and microhardness using RSM.
2. From the results, it was concluded that running with a powder feed rate of 45 gm/min, an oxygen flow rate of 240 slpm, a spray distance of 6.5 inches and LPG flow rate of 60 slpm gives vol % of porosity = 1.3 (Minimum) and a value of microhardness = 1267 HV (Maximum) in the coating.
3. F value results of ANOVA confirm that the fuel flow rate (O) has a higher effect on the porosity level and the microhardness of the HVOF coating than that of other parameters.
4. The results also confirm that porosity and hardness always exhibit an inverse relationship.

References

1. Vaßen, R.; Bakan, E.; Gatzen, C.; Kim, S.; Mack, D.E.; Guillon, O. Environmental Barrier Coatings Made by Different Thermal Spray Technologies. *Coatings* **2019**, *9*, 784. [CrossRef]
2. Joshi, S.; Nylen, P. Advanced Coatings by Thermal Spray Processes: A review. *Technologies* **2019**, *7*, 79. [CrossRef]
3. Romanov, D.; Moskovskii, S.; Konovalov, S.; Sosnin, K.; Gromov, V.; Ivanov, Y. Improvement of copper alloy properties in electro-explosive spraying of ZnO-Ag coatings resistant to electrical erosion. *J. Mater. Res. Technol.* **2019**, *8*, 5515–5523. [CrossRef]
4. Mohankumar, A.; Duraisamy, T.; Chidambaramseshadri, R.; Pattabi, T.; Ranganathan, S.; Kaliyamoorthy, M.; Balachandran, G.; Sampathkumar, D.; Rajendran, P.R. Enhancing the Corrosion Resistance of Low Pressure Cold Sprayed Metal Matrix Composite Coatings on AZ31B Mg Alloy through Friction Stir Processing. *Coatings* **2022**, *12*, 135. [CrossRef]
5. Kannan, M.; Duraisamy, T.; Pattabi, T.; Mohankumar, A. Investigate the corrosion properties of stellite coated on AZ91D alloy by plasma spray technique. *Therm. Sci.* **2021**, 209. [CrossRef]
6. Ashokkumar, M.; Thirumalaikumarasamy, D.; Thirumal, P.; Barathiraja, R. Influences of Mechanical, Corrosion, erosion and tribological performance of cold sprayed Coatings A review. *Mater. Today Proc.* **2021**, *46*, 7581–7587. [CrossRef]
7. Mathanbabu, M.; Thirumalaikumarasamy, D.; Thirumal, P.; Ashokkumar, M. Study on thermal, mechanical, microstructural properties and failure analyses of lanthanum zirconate based thermal barrier coatings: A review. *Mater. Today Proc.* **2021**, *46*, 7948–7954. [CrossRef]
8. Straffelini, G.; Federici, M. HVOF Cermet Coatings to Improve Sliding Wear Resistance in Engineering Systems: A review. *Coatings* **2020**, *10*, 886. [CrossRef]
9. Brezinová, J.; Guzanová, A.; Tkáčová, J.; Brezina, J.; Ľachová, K.; Draganovská, D.; Pastorek, F.; Maruschak, P.; Prentkovskis, O. High Velocity Oxygen Liquid-Fuel (HVOLF) Spraying of WC-Based Coatings for Transport Industrial Applications. *Metals* **2020**, *10*, 1675. [CrossRef]
10. Tilger, M.; Biermann, D.; Abdulgader, M.; Tillmann, W. The Effect of Machined Surface Conditioning on the Coating Interface of High Velocity Oxygen Fuel (HVOF) Sprayed Coating. *J. Manuf. Mater. Process.* **2019**, *3*, 79. [CrossRef]
11. Wu, M.; Pan, L.; Duan, H.; Wan, C.; Yang, T.; Gao, M.; Yu, S. Study on Wear Resistance and Corrosion Resistance of HVOF Surface Coating Refabricate for Hydraulic Support Column. *Coatings* **2021**, *11*, 1457. [CrossRef]
12. Javed, M.A.; Ang, A.S.M.; Bhadra, C.M.; Piola, R.; Neil, W.C.; Berndt, C.C.; Leigh, M.; Howse, H.; Wade, S.A. Corrosion and mechanical performance of HVOF WC-based coatings with alloyed nickel binder for use in marine hydraulic applications. *Surf. Coat. Technol.* **2021**, *418*, 127239. [CrossRef]
13. Vignesh, S.; Shanmugam, K.; Balasubramanian, V.; Sridhar, K. Identifying the optimal HVOF spray parameters to attain minimum porosity and maximum hardness in iron based amorphous metallic coatings. *Def. Technol.* **2017**, *13*, 101–110. [CrossRef]
14. Karthikeyan, S.; Balasubramanian, V.; Rajendran, R. Developing empirical relationships to estimate porosity and microhardness of plasma-sprayed YSZ coatings. *Ceram. Int.* **2014**, *40*, 3171–3183. [CrossRef]
15. Vignesh, S.; Balasubramanian, V.; Sridhar, K.; Thirumalaikumarasamy, D. Slurry Erosion Behavior of HVOF-Sprayed Amorphous Coating on Stainless Steel. *Met. Microstruct. Anal.* **2019**, *8*, 462–471. [CrossRef]
16. Prasad, R.V.; Rajesh, R.; Thirumalaikumarasamy, D.; Vignesh, S.; Sreesabari, S. Sensitivity analysis and optimisation of HVOF process inputs to reduce porosity and maximise hardness of WC-10Co-4Cr coatings. *Sādhanā* **2021**, *46*, 149. [CrossRef]
17. Ribu, D.C.; Rajesh, R.; Thirumalaikumarasamy, D.; Vignesh, S. Influence of rotational speed, angle of impingement, concentration of slurry and exposure time on erosion performance of HVOF sprayed cermet coatings on 35CrMo steel. *Mater. Today Proc.* **2021**, *46*, 7518–7530. [CrossRef]
18. Thirumalvalavan, S.; Senthilkumar, N. Experimental Investigation and Optimization of HVOF Spray Parameters on Wear Resistance Behaviour of Ti-6Al-4V Alloy. *Comptes Rendus L'academie Bulg. Sci.* **2019**, *72*, 664–673. [CrossRef]
19. Qiao, L.; Wu, Y.; Hong, S.; Long, W.; Cheng, J. Wet abrasive wear behavior of WC-based cermet coatings prepared by HVOF spraying. *Ceram. Int.* **2020**, *47*, 1829–1836. [CrossRef]
20. Murugan, K.; Ragupathy, A.; Balasubramanian, V.; Sridhar, K. Optimization of HVOF spray parameters to attain minimum porosity and maximum hardness in WC-10 Ni-4 Cr coatings. *Surf. Coat. Technol.* **2014**, *247*, 90–102. [CrossRef]
21. Thermsuk, S.; Surin, P. Optimization Parameters of WC-12Co HVOF Sprayed Coatings on SUS 400 Stainless Steel. *Procedia Manuf.* **2019**, *30*, 506–513. [CrossRef]
22. Baumann, I.; Hagen, L.; Tillmann, W.; Hollingsworth, P.; Stangier, D.; Schmidtmann, G.; Tolan, M.; Paulus, M.; Sternemann, C. Process characteristics, particle behavior and coating properties during HVOF spraying of conventional, fine and nanostructured WC-12Co powders. *Surf. Coat. Technol.* **2020**, *405*, 126716. [CrossRef]

23. Liu, S.; Wu, H.; Xie, S.; Planche, M.-P.; Rivolet, D.; Moliere, M.; Liao, H. Novel liquid fuel HVOF torches fueled with ethanol: Relationships between in-flight particle characteristics and properties of WC-10Co-4Cr coatings. *Surf. Coat. Technol.* **2021**, *408*, 126805. [CrossRef]

24. Guzanová, A.; Brezinová, J.; Draganovská, D.; Maruschak, P.O. Properties of coatings created by HVOF technology using micro-and nano-sized powder. *Koroze Ochr. Mater.* **2019**, *63*, 86–93. [CrossRef]

25. Guo, X.; Planche, M.-P.; Chen, J.; Liao, H. Relationships between in-flight particle characteristics and properties of HVOF sprayed WC-CoCr coatings. *J. Mater. Process. Technol.* **2014**, *214*, 456–461. [CrossRef]

26. Yuan, J.; Ma, C.; Yang, S.; Yu, Z.; Li, H. Improving the wear resistance of HVOF sprayed WC-Co coatings by adding submicron-sized WC particles at the splats' interfaces. *Surf. Coat. Technol.* **2016**, *285*, 17–23. [CrossRef]

27. Mathivanan, K.; Thirumalaikumarasamy, D.; Ashokkumar, M.; Deepak, S.; Mathanbabu, M. Optimization and prediction of AZ91D stellite-6 coated magnesium alloy using Box Behnken design and hybrid deep belief network. *J. Mater. Res. Technol.* **2021**, *15*, 2953–2969. [CrossRef]